Tracer impurity transport inside an IDB plasma of LHD

Naoki TAMURA, Kuninori SATO, Pavel R GONCHAROV, Hisamichi FUNABA, Yuri L IGITKHANOV, Shigeru SUDO, Ichihiro YAMADA, Kazumichi NARIHARA, Kenji TANAKA, Clive MICHAEL, Kazuo KAWAHATA, Shinji YOSHIMURA, Byron J PETERSON, Ryuichi SAKAMOTO, Masahiro KOBAYASHI, Hiroshi YAMADA, Nobuyoshi OYABU, Akio KOMORI and LHD Experimental Group

National Institute for Fusion Science, Toki 509-5292, Japan

Recently, in LHD, extremely high-density region accompanied with an Internal Diffusion Barrier (IDB) has been established by optimizing a pellet fueling and a magnetic configuration. In order to understand impurity transport inside the IDB plasma of LHD, a tracer-encapsulated solid pellet (TESPEL), which can deposit a tracer impurity locally inside the plasma, injection into the IDB plasma has been performed. In this experiment, titanium (Ti) particles are loaded into the TESPEL as a tracer. The local deposition of the Ti tracer impurity inside the IDB is successfully achieved with the help of the TESPEL technique, which is confirmed by an optical measurement. Considering temporal change in both electron density and electron temperature, temporal behavior of line emissions from the Ti tracer impurity ions measured by a vacuum ultra violet spectrometer indicates the Ti tracer impurity ions seems to be accumulated inside the IDB.

Keywords: impurity transport, TESPEL, local tracer deposition, ultrahigh density, internal diffusion barrier

1. Introduction

Understanding and control of impurity transport in magnetically confined plasmas is still an important issue for achieving a practical fusion reactor, since impurities can significantly influence the reactor performance through such effects as radiative losses, radiative instabilities, fuel dilution and so on. Especially when an “impurity accumulation” takes place in the core plasma, these problems become more acute. Thus impurity transport study has been performed diligently in many tokamaks and stellarators/heliotrons so far [1-6].

In Large Helical Device (LHD) [7], ultrahigh density region (the maximum density in the region is up to 1 x 10^{21} m^{-3}) accompanied with an Internal Diffusion Barrier (IDB) has been established by optimizing a pellet fueling and a magnetic configuration [8, 9]. One of the important points to be clarified for the IDB plasmas is whether the IDB causes an impurity accumulation or not. So far, the performance degradation of the IDB plasmas due to the impurity accumulation has not been observed despite the existence of a negative radial electric field. In LHD, a tracer-encapsulated solid pellet (TESPEL) [5, 10], which allow us to obtain a three-dimensionally localized deposition of the tracer impurity inside the plasma, has been utilized for impurity transport study. When a low-level transport such as an internal transport barrier for impurity is established inside the plasma, the TESPEL technique has a great advantage in the study of the transport inside and in the vicinity of that region, since it takes longer for an intrinsic impurity influx from the plasma facing components to arrive at there.

So TESPEL injection has been tried to investigate impurity transport inside the IDB plasma.

2. Experimental setup

The LHD with a heliotron type magnetic configuration is the world’s largest helical device and has superconducting l/m = 2/10 helical coils and 3 pairs of superconducting poloidal coils. In this experiment, the position of a magnetic axis R_{ax} is 3.85 m and the magnetic field strength at the axis is 2.571 T. The plasma was started up by an electron cyclotron heating and heated additionally by a tangential neutral beam injection (NBI). And then the ultrahigh core electron density accompanied with the IDB is obtained by a multiple solid hydrogen pellet injection [11], in which the size of the pellet and the time interval of injection are optimized. In order to introduce a tracer impurity inside the IDB, a TESPEL is utilized. As a tracer impurity, titanium (Ti) particles, the total amount of which is approximately 2 x 10^{17} particles, are loaded into the TESPEL. The TESPEL injector is installed on the equatorial plane at Port 3-O of LHD and the TESPEL is injected from the outboard side of the LHD plasma. A detailed radial profile of electron density n_e and electron temperature T_e is measured with a Thomson scattering system. Total radiated power P_{rad} is measured by a wide

author's e-mail: ntamura@LHD.nifs.ac.jp

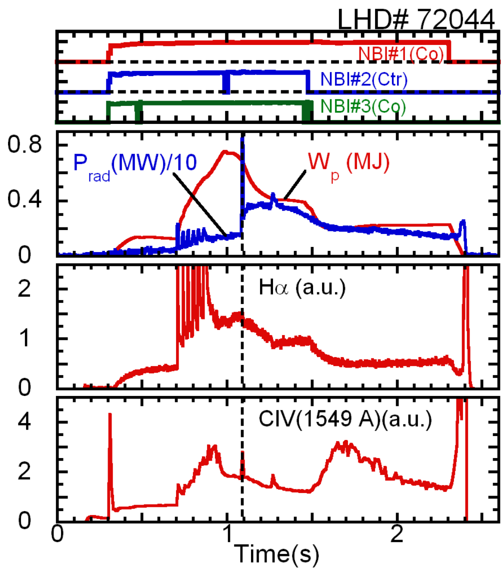

Fig. 1 Typical waveforms of the IDB plasma with TESPEL injection. A vertical dashed line denotes the TESPEL injection time, $t \sim 1.09$ s.

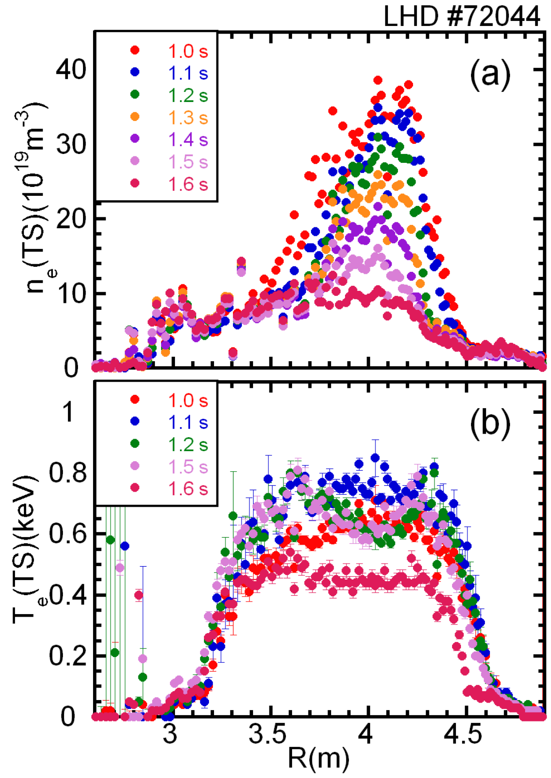

Fig. 2 Radial profile of (a) electron density n_e and (b) electron temperature T_e measured by the Thomson scattering system. TESPEL is injected at $t \sim 1.09$ s.

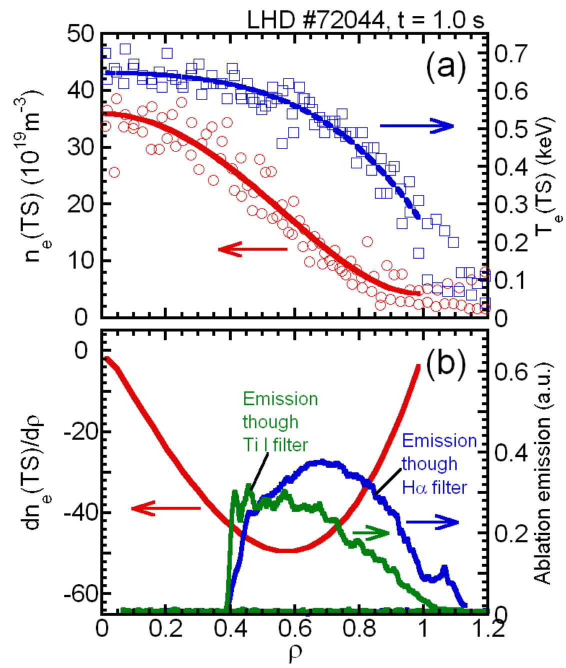

Fig. 3 (a) Electron density and electron temperature measured by the Thomson scattering system at t = 1.0 s before the TESPEL injection as a function of normalized averaged minor radius and (b) electron density gradient and TESPEL ablation emissions as a function of the normalized averaged minor radius. Ti-tracer would be deposited between ρ = 0.4 and ρ = 0.5.

angle metal foil bolometer, which is installed at the same port (Port 3-O) as the TESPEL injector and plasma radiation light is done by absolute extreme ultra violet silicon photodiode (AXUVD) arrays, which are installed at Port 3.5U and 4-O on a semi-tangential cross-section in LHD [12]. The temporal behavior of the emissions in a vacuum ultra violet (VUV) domain from the Ti tracer ions is measured by a Schwob-Fraenkel soft x-ray multi-channel spectrometer (SOXMOS, typical exposure time ~ 50 ms).

3. Tracer Impurity Injection into IDB Plasma

Figure 1 shows typical waveforms of the IDB plasma with the TESPEL injection. In this discharge, as can be clearly seen in the Hα signal, the multiple solid hydrogen pellet injection is performed from t = 0.71 s to t = 0.86 s and then the ultrahigh density region with the IDB is established. And then The TESPEL is injected at $t \sim 1.09$ s. At this time there is a very sharp peak in the P_{rad}. This is because the wide angle bolometer, which is installed at the same port as the TESPEL injector, can also observe the emissions from the TESPEL ablation cloud. After this sharp peak, the P_{rad} is higher than that during the period from the end of the multiple pellet injection through until the time of the TESPEL injection (the period of the IDB plasma without the Ti tracer impurity) and remains at the higher level for about 300 ms. And then the P_{rad} is gradually decreased, which is started before NBIs (#2 and #3) are turned off. At about t = 1.3 s, a small peak can be seen in the signals of the P_{rad} and the C IV. This has no relationship to the TESPEL injection. This might be because carbon flakes fell into the plasma.

Figure 2 shows radial profiles of n_e and T_e during the period from t = 1.0 s to t = 1.6 s. The ultrahigh density region fades gradually during this period and vanished completely at t = 1.6 s. The TESPEL injection, which is done at $t \sim$ 1.09 s, seems to have little impact on the IDB. After the TESPEL injection (from t = 1.2 s), the T_e profile becomes the hollow profile, which remains until t = 1.5 s. This could be ascribed to the accumulation of the Ti tracer impurity inside the IDB.

Figure 3 (a) shows n_e and T_e at t = 1.0 s before the TESPEL injection as a function of the normalized averaged minor radius. To project the R-coordinate on the ρ-coordinate, the three-dimensional free boundary MHD equilibrium code VMEC is used. As seen in Fig. 3(a), the ultrahigh density region can be seen in a wide region of the plasma (The value of n_e with over 1.0 x 10^{20} m^{-3} is seen inside $\rho \sim$ 0.75.) As can be seen in Fig. 3(b), the TESPEL penetrates deeply inside the IDB plasma and consequently the Ti tracer is deposited between ρ = 0.4 and ρ = 0.5. Thus the deposition of Ti tracer impurity inside the IDB is successfully achieved.

4. Temporal behavior of tracer impurity deposited inside the IDB

Figure 4(a) shows temporal evolutions of sight-line-integrated signals of AXUVD arrays, which are not equipped with any optical filters. Just after the TESPEL injection, the signals of the all channel in both arrays are increased drastically. Shortly thereafter the signals of the all channels except the channel 13 are decreased gradually (the signal of the channel 13 in both arrays is increased more and sustained.). Considering the geometry of line-of-sight of AXUVD arrays as shown in fig. 4(b), the profile of plasma radiation light become extremely peaky after the TESPEL injection. Moreover, taking the gradual decrease in n_e and no change in T_e during the period from t = 1.2 s to t = 1.5 s into account, the signals of AXUVD arrays suggests that the Ti tracer impurity is accumulated inside the IDB. Figure 5 shows temporal behavior of VUV emissions (Ti XV (O-like), 11.50 nm and Ti XI (Mg-like), 8.772 nm) from the Ti tracer ions measured with the SOXMOS. Just after the TESPEL injection, Both VUV emissions are increased rapidly and then are decreased gradually. When two NBIs (#2 and #3) are turned off at t = 1.5 s, the Ti XV intensity is drastically decreased, but Ti XI is not. Taking the gradual change in n_e and no change in T_e during the period from t = 1.2 s and t = 1.5 s into account, the experimental results obtained by the VUV spectrometer again suggest that the Ti tracer impurity deposited inside the ultrahigh core density region is accumulated.

In order to estimate quantitatively impurity transport inside the ultrahigh core density region, impurity

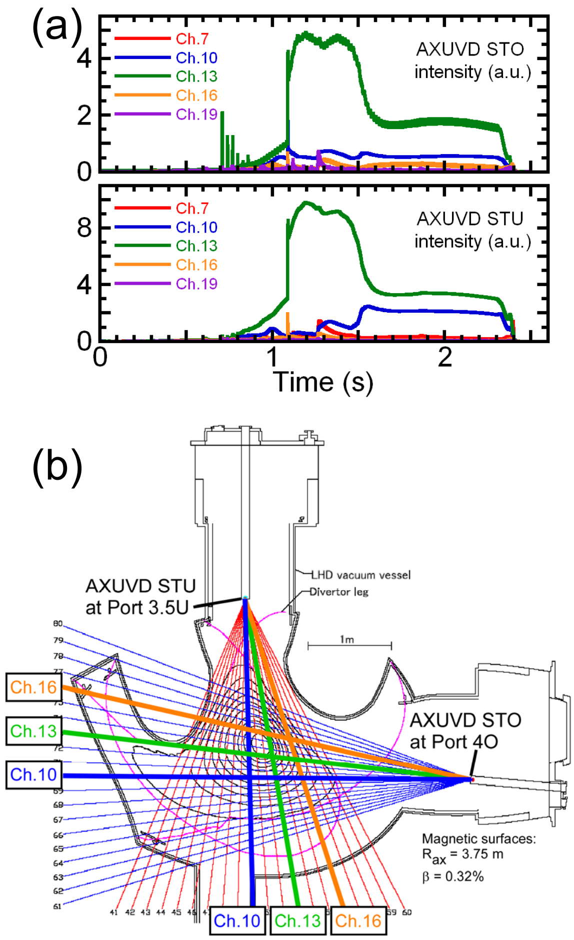

Fig. 4 (a) Temporal evolutions of AXUVD arrays' signals. TESPEL injection time is $t \sim$ 1.09 s. (b) Line-of-sight of corresponding AXUVD arrays. Displayed magnetic surface is just an example.

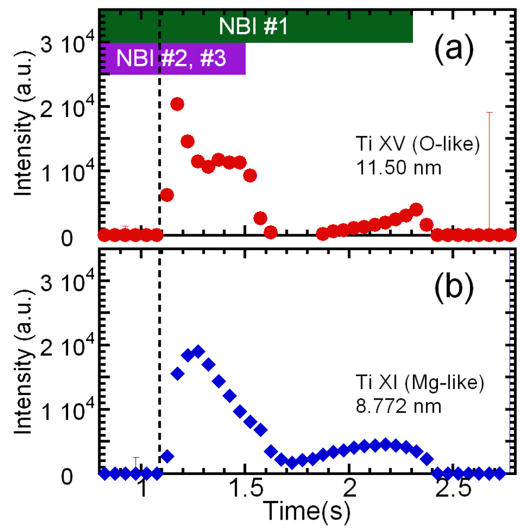

Fig. 5 Temporal evolutions of (a) Ti XV (O-like, 11.50 nm) and (b) Ti XI (Mg-like, 8.772 nm) measured with a VUV spectrometer. NBI #2 and #3 turned off at t = 1.5 s and NBI #1 turned off at t = 2.3 s.

transport analysis, taking temporal change in n_e and T_e into account, will be performed with 1-D transport code, such as MIST and Strahl. Further TESPEL injection experiments will be performed to obtain the tracer deposition inside and outside the IDB, allowing us to know qualitatively the effect of IDB on impurity transport.

5. Concluding remarks

Recently, in LHD, the ultrahigh core electron density accompanied with the internal diffusion barrier has been obtained. In order to investigate impurity transport inside the IDB, Ti tracer impurity injection into the ultrahigh core density region was tried by means of TESPEL. The local deposition of the Ti tracer impurity in the ultrahigh core density region is successfully achieved. Temporal behavior of the line emissions from the Ti tracer impurity ion has been clearly observed with the VUV spectrometer. Taking temporal change in both n_e and T_e into account, the Ti tracer impurity ions seems to be accumulated inside the IDB.

Acknowledgement

The authors acknowledge all of the technical staff of NIFS for their excellent support. They also would like to thank Prof. O. Motojima (Director of NIFS) for his continuous encouragement. This work is partly supported by a Grant-in-Aid for Scientific Research (B) (No. 19340179) from Japan Society for the Promotion of Science, a Grant-in-Aid for Young Scientists (B) (No. 19740349) from MEXT Japan and a budgetary Grant-in-Aid No. NIFS07ULHH510 and NIFS07ULHH524 of the National Institute for Fusion Science.

References

[1] R. Guirlet *et al*., Nucl. Fusion **48**, B63 (2006).
[2] D. Stutman et al., Phys. Plasma **10**, 4387 (2003).
[3] K. Ida *et al*., Plasma Phys. Control. Fusion **45**, 1931 (2003).
[4] Y. Nakamura *et al*., Nucl. Fusion **43**, 219 (2003).
[5] N. Tamura *et al*., Plasma Phys. Control. Fusion **45**, 27 (2003).
[6] H. Nozato et al., Phys. Plasmas **13**, 092502 (2006).
[7] O. Motojima *et al*., Phys. Plasmas **6**, 1843 (1999).
[8] H. Yamada *et al*., 34th EPS Conf. on Plasma Physics (Warsaw, Poland) (2007) I4.004.
[9] R. Sakamoto *et al*, this conference.
[10] S. Sudo *et al*., Plasma Phys. Control. Fusion **44**, 129 (2002).
[11] H. Yamada *et al*., Fusion Eng. Des. **49-50**, 915 (2000).
[12] B. J. Peterson *et al*., Plasma Phys. Control. Fusion **45**, 1167 (2003)